Journal of Fluorescence, Vol. 6, No. 2, 1996

Diffusion-Enhanced Resonance Energy Transfer Shows that Linker-DNA Accessibility Decreases During Salt-Induced Chromatin Condensation

R. Labarbe,[1] S. Mignon,[1] S. Flock,[1] and C. Houssier[1,2]

Received July 24, 1995; accepted May 7, 1996

Accessibility of linker-DNA chromatin during salt-induced condensation of chicken erythrocytes chromatin was studied by diffusion-enhanced resonance energy transfer. A terbium complex was covalently bound to linker-DNA and fluorescein molecules bound to latex particles with diameters ranging from 14 to 2470 nm were used as acceptor. The accessibility of linker-DNA to molecules with a diameter superior to 14 nm diminished during condensation, but for an acceptor diameter of 14 nm or less, no accessibility variation was observed. It can be concluded that (1) linker-DNA is located inside the fiber when chromatin is in the condensed state, (2) chromatin condensation can prevent the approach to DNA due to steric hindrance, (3) salt-induced chromatin condensation is a gradual process, and (4) condensed chromatin models containing a central cavity are more likely.

KEY WORDS: Chromatin; condensation; energy transfer; terbium; psoralen.

INTRODUCTION

One of the many mechanisms that control the regulation of genes expression in nuclei is the degree of chromatin condensation. The heterochromatin, the region of chromatin that is in a condensed state in interphase cells, is believed to be composed essentially of unexpressed genes. Indeed, the translocation of an active gene near a heterochromatic domain can result in its repression, an effect which is called position-effect variegation. Reuter *et al.*[1] showed that in *Drosophila* a zinc finger protein is a controlling agent for the formation of heterochromatin and thus modulates the variegation effect. *In vitro* Hansen and Wolffe[2] showed that the compaction of arrays of nucleosomes induced by Mg^{2+} inhibits the transcription of *Xenopus* 5S RNA genes. Kamakaka and Thomas[3] showed that, in chicken erythrocytes, the once active β-globin gene is partially depleted of H1 and H5 histones relative to inactivated genes. The H1 and H5 histones, which are known to stabilize the condensed structures of chromatin,[4] are responsible for eukaryotic gene repression, possibly through the formation of condensed chromatin structures.[5] These observations led to the conclusion that chromatin condensation has a major role in repressing genes transcription, possibly by preventing transcription proteins from approaching the DNA by steric hindrances. It thus appears interesting to determine quantitatively the accessibility of DNA in chromatin toward molecules of different sizes at various degrees of chromatin condensation.

Resonance energy transfer measurements have long been used in the field of biomolecular structure and dy-

[1] Laboratoire de Chimie Macromoléculaire et Chimie Physique, Institut de Chimie, Sart Tilman (B6), Université de Liège, B-4000 Liège, Belgium.

[2] To whom correspondence should be addressed.

[2] Abbreviations used: DTPA, diethylene tetramine pentacetic acid; FDL-DERET, fast diffusion limit of diffusion-enhanced resonance energy transfer; Pso–Tb, psoralen–terbium complex; PAS, paraamino salicylic acid; TREF, time-resolved emission of fluorescence.

1053-0509/96/0600-0107$09.50/0

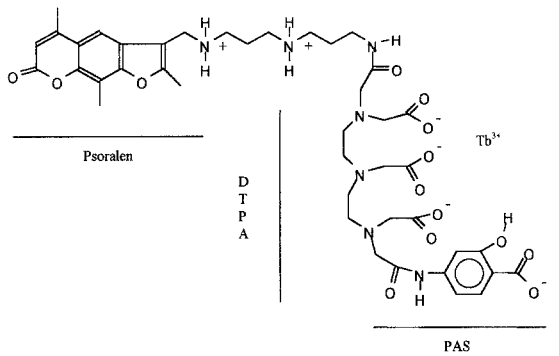

Fig. 1. Psoralen–terbium complex (Pso–Tb). The different constituents of the molecule are outlined: PAS, paraamino salicylic acid; DTPA, diethylenetetraminepentacetic acid.

namics to measure distances (for review, see Ref. 6). In this work, we chose a terbium complex covalently attached to linker-DNA of chicken erythrocytes chromatin as fluorescent donor molecule. The acceptor particles are polystyrene Fluospheres labeled with fluorescein and having diameters ranging from 14 to 2.47 μm. We observed the variation of the Förster energy transfer rate constant during chromatin condensation induced by an increase in the sodium chloride concentration and related the constant to the distance of closest approach between the fluorescent terbium donor and the fluorescein acceptor, i.e., to the accessibility of linker-DNA for the Fluospheres.

EXPERIMENTAL

Terbium Complex $Tb(EDTA)^-$

$Tb(EDTA)^-$ complex was prepared by the addition of an excess of EDTA to $TbCl_3 \cdot 6H_2O$ in aqueous solution. The complex was purified by ion-exchange chromatography on an AG1X8 column with elution by an ammonium acetate gradient (0.01 to 4 *M*, pH 6.8). The identification of the complex in the collected fractions was carried out by fluorescence measurements. The collected solution was then freeze-dried and kept at 4°C.

Terbium Complex Psoralene–Terbium

The 4"-{9‴-[(4-carboxy-3-hydroxyphenyl)-acetamido)-3‴,6‴,9‴-(triacetyl)-3",6‴,9‴-triazanonamido]-2", 6"-diazanonyl}-4,5',8-trymethyl psoralen–terbium complex (Pso–Tb; Fig. 1) was synthesized by a modified Oser reaction [7,8] and is the fluorescent donor molecule. It is composed of a psoralen moiety linked to a terbium complex (PAS–DTPA–Tb) via a diazanonyl linker. All reactions were carried out in the dark, as psoralen is photosensitive. The product was purified by chromatography on a Bio-Rad AG50WX8 column with elution by 1 m*M* NH_4Cl and was detected by measurement of the absorbance at 210 nm. The collected solution was freeze-dried. Pso–Tb is a white powder and was kept in the dark. Characterization of the product was made by FT-IR spectroscopy, mass spectrometry, and fluorescence spectroscopy (not shown).

Chromatin Preparation

Chicken erythrocyte chromatin was prepared from chicken blood as described previously.[9] The chromatin can be stored in sodium cacodylate buffer, pH 6.5, at 4°C for 10 days.

Covalent Fixation of Psoralen–Terbium Complex to DNA and Chromatin

A Pso–Tb solution was mixed with a DNA or chromatin solution so that the ratio [DNA or chromatin]/[Pso–Tb] is 100 (polymer concentration is expressed in mole of nucleotides per litre). The solution was equilibrated for 1 h at 0°C in the dark. The photocovalent reaction was initiated by irradiation of the solution with a near-UV light at a 366-nm wavelength at 0°C. The 366-nm radiation was isolated from an Hamamatsu xenon lamp (Model L-2569) by a blue filter which removed the lamp emission above 455 nm and below 340 nm. The solution was dialyzed three times against 1 m*M* sodium cacodylate buffer at pH 6.5 in order to remove non-covalently bound molecules.

Fluospheres

The Fluospheres were purchased from Molecular Probes Inc. (Eugene, OR). They are constituted of a nonporous polystyrene spherical core and a slightly porous surface constituted of grafted polymer containing negatively charged carboxylic acid groups, thus reducing the hydrophobic character of the latex spheres and preventing them from histone protein adsorption. The high level of fluorescein labeling of the spheres gives rise to a high energy transfer from terbium. The diameters of the spheres were 14, 93, 282, 977, and 2470 nm. The Fluospheres can be used in buffers containing up to 1 *M* univalent salt without precipitation and their visible absorption maximum is located at 490 nm. The Fluos-

pheres were dissolved in sodium cacodylate buffer, pH 6.5, and the solution was sonicated before use in order to disrupt aggregates.

Lifetime Measurements

Fluorescence lifetimes were measured with an Edinburgh (Scotland) photocounting instrument, Model 199S, equipped with a microsecond xenon flashlamp, Model 199XF. Excitation and emission wavelengths were set at 460 and 490 nm, respectively. The lifetimes were calculated from the fluorescence decay curves by the least-squares method using software provided by the IBH Company (Glasgow, Scotland).

Principle of the Accessibility Measurements

Förster showed that a fluorescent donor molecule can transfer its energy to an acceptor molecule via a dipole–dipole interaction.[10] The resonance energy transfer occurs with a static transfer rate constant k_2 (M^{-1} s^{-1}) given by

$$k_2 = 8.71 \cdot 10^{23} J \kappa^2 n^{-4} \Phi_0 \tau_0^{-1} r^{-6} \tag{1}$$

where n is the refraction index of the solution, Φ_0 and τ_0 are, respectively, the quantum yield and the lifetime (s) of the donor in the absence of acceptor, κ is a factor depending on the relative orientation of the donor and acceptor transition moments, and r is the distance (Å) between donor and acceptor. When the donor and acceptor are free to rotate, the orientation factor is equal to 2/3. The overlap integral $J(M^{-1}$ $cm^3)$ is defined as

$$J = \frac{\int F(\lambda) \cdot \varepsilon(\lambda) \cdot \lambda^4 \cdot d\lambda}{\int F(\lambda) \cdot d\lambda} \tag{2}$$

where $F(\lambda)$ is the fluorescence intensity of the donor at wavelength λ and $\varepsilon(\lambda)$ is the extinction coefficient (M^{-1} cm^{-1}) of the acceptor at the same wavelength.

Equation (1) can be rewritten as

$$k_2 = \frac{1}{\tau_0} \left(\frac{R_0}{r} \right)^6 \tag{3}$$

where R_0 (Å), the critical Förster distance, is equal to

$$R_0 = 9.79 \cdot 10^3 \, (J \kappa^2 \Phi_0 n^{-4})^{1/6} \tag{4}$$

When the donor fluorescence lifetime is sufficiently long, the acceptor has enough time to diffuse toward the donor before donor deexcitation by fluorescence and so the energy transfer is enhanced. In the case of very rapid diffusion, the energy transfer will reach its maximum value: the system is in the fast diffusion limit of diffusion enhanced resonance energy transfer (FDL-DERET) and the fluorescence lifetime τ of the donor is related to the acceptor concentration $[A]$ by[10]

$$\frac{1}{\tau} = \frac{1}{\tau_0} + k_d[A] \tag{5}$$

where k_d is the dynamic transfer rate constant.

In order to study the accessibility of linker-DNA in chicken erythrocytes chromatin toward molecules of different sizes, we have used a fluorescent donor (Pso–Tb) bound to the linker-DNA and an acceptor bound to spherical particles of variable size. A measurement of the Förster transfer rate constant k_d, under the FDL-DERET conditions, will give an estimation of the variation of linker-DNA accessibility as salt-induced chromatin condensation occurs.

If the donor is bound at the center of a cylinder of radius R_d and the acceptor at the center of a sphere of radius R_a, then the dynamic transfer rate constant (in FDL-DERET) must be computed by integrating the static transfer rate constant k_2 over all orientations and distances between donor and acceptor,[11] leading to

$$k_d = \frac{10^{-27} N_A \pi^2 R_0^6}{4 \tau_0 d^3} \tag{6}$$

where d (Å) is the distance of closest approach between the donor and the acceptor ($d = R_d + R_a$) and N_A is Avogadro's number.

The distance of closest approach is related to the accessibility of the donor toward the acceptor. The smaller the accessibility, the greater is the distance of closest approach and the smaller is the transfer rate constant. A measurement of the donor lifetime at different acceptor concentrations will allow the determination of transfer rate constant and thus gives an estimation of the accessibility of the donor.

It can be shown (see Appendix) that when the acceptor is not at the center of the sphere but uniformly distributed over the sphere (as in the Fluospheres), Eqs. (3) to (6) are still valid. If donors and acceptors are charged, the expression of the static transfer rate constant must be modified to take into account the repulsion or attraction between the two molecules. Equation (1) must be multiplied by an exponential factor $e^{(-\omega(r)/kT)}$, where $\omega(r)$ is the potential of the mean force between the two charges, k is the Boltzmann constant, and T is the absolute temperature.[12]

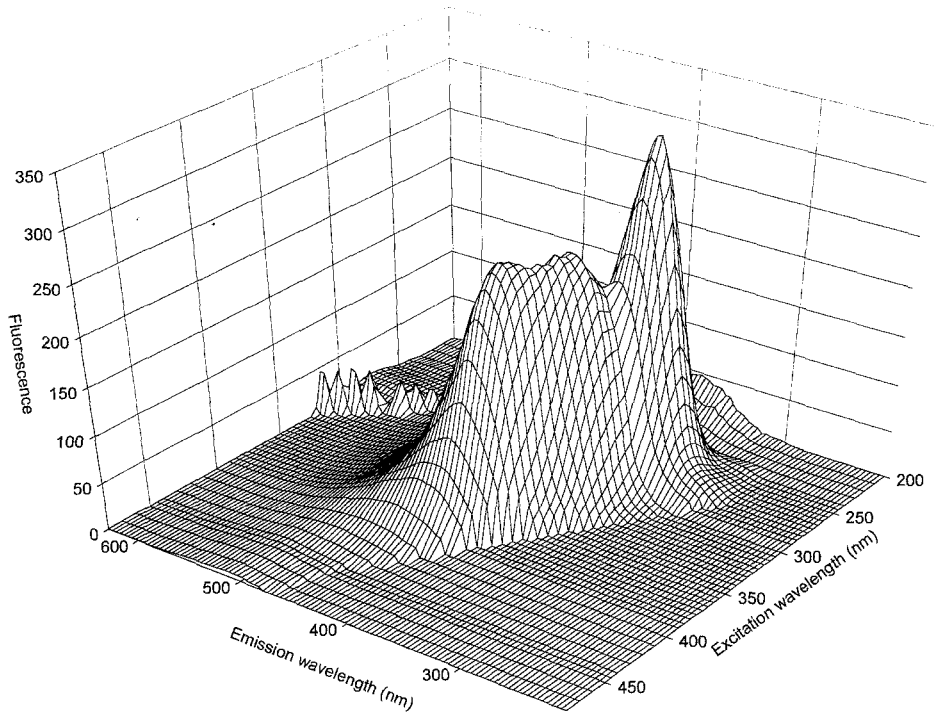

Fig. 2. Total fluorescence spectrum of the psoralen–terbium complex. Horizontal axis represents the excitation and emission wavelengths. Vertical axis is the fluorescence intensity.

RESULTS

The psoralen moiety of the Pso–Tb donor complex (Fig. 1) intercalates between the bases pairs of DNA and can photocovalently cross-link DNA at thymine sites by irradiation at 366 nm.[13] It appeared necessary to bind covalently the probe to the DNA in order to prevent its expulsion from its intercalation site when the chromatin condensation is induced by salt addition. The psoralen shows a preference for fixation at 5'-TA sequences relative to 5'-AT sequences.[14] Cross-linking of psoralen to DNA does not appreciably perturb the DNA structure. It lengthens the DNA only by about the equivalent of 1 bp per bound adduct.[16] The circular dichroism spectra of DNA and psoralen–DNA photoadduct are very similar (data not shown); we can thus be confident that the structure of the DNA is not greatly affected by the fixation of the probe. It shows a preference for certain domains of chromatin: when the ratio [chromatin]/[Pso–Tb] is greater than 100, the psoralen is bound almost exclusively to linker-DNA.[15] At so low an intercalator concentration it was shown[16] that 90% of the DNA in chromatin is protected from psoralen binding and thus the chromatin retains its higher-order structure and no perturbation of its condensation by the psoralen is to be feared.

The diameters of the acceptor Fluospheres simulate a large range of protein sizes. The spheres are negatively charged, so that they do not adsorb on DNA and remain free to diffuse in the solution. The advantages of using synthetic polymers relative to proteins probes are (1) the better control of the diameter and size dispersion of the probe, (2) the absence of positive charges that could lead to DNA binding, (3) the absence of any sequence specificity, and (4) the stability toward ionic strength variations.

Spectral Properties of Pso–Tb

The extinction coefficient of Pso–Tb is 290 M^{-1} cm^{-1} at 280 nm. The fluorescence emission spectra of free Pso–Tb for various excitation wavelengths are shown in Fig. 2. In this spectrum, one horizontal axis represents the excitation wavelength, the other horizontal axis represents the emission wavelength, and the vertical axis is the fluorescence emission intensity. A slice in the graph parallel to the emission axis represents a classical fluorescence excitation spectrum and a slice parallel to the excitation axis represents a classical emission spectrum. The group of peaks above 500 nm (emission) are the second-order scattering peaks. For clarity, the first-

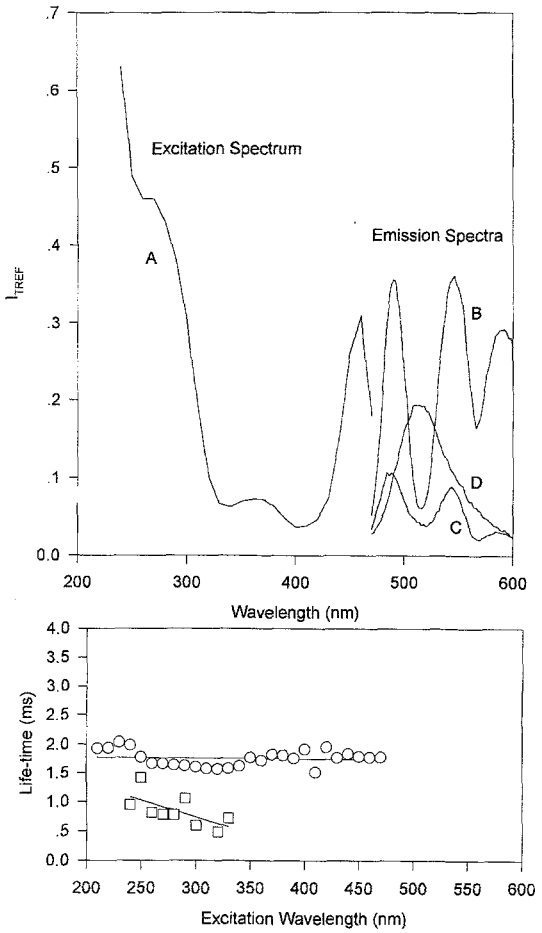

Fig. 3. Top: Time resolved emission of fluorescence spectra (TREF) of Pso–Tb in the absence and in the presence of fluorescein. I_{TREF} represents the integrated fluorescence from 0.88 ms after the lamp flash up to infinite time. (A) TREF excitation spectrum of Pso–Tb (emission, 490 nm). (B) TREF emission spectrum of Pso–Tb (excitation, 460 nm). (C) TREF emission spectrum of Pso–Tb with 10^{-5} *M* fluorescein (excitation, 460 nm). (D) TREF emission spectrum of Pso–Tb with $5{\cdot}10^{-5}$ *M* fluorescein (excitation, 460 nm). Bottom: Fluorescence lifetimes of Pso–Tb as a function of the excitation wavelength (emission, 490 nm).

order scattering peaks have been removed. By comparison with the fluorescence spectrum of psoralen (Pso), paraamino salicylic acid (PAS), and Tb^{3+}, it can be concluded that the fluorescence spectrum of Pso–Tb is the result of the superposition of the fluorescence of each of its separate components. The fluorescence originates from the psoralen part for excitation between 250 and 300 nm and from PAS between 320 and 400 nm. As the fluorescence of Tb^{3+} is superimposed on the fluorescence of each of the organic components, it is not possible to clearly identify the characteristic emission peaks of terbium (emission at 490, 545, and 580 nm). In order to select the appropriate excitation–emission wavelengths for lifetime measurements, it would be useful to isolate the fluorescence emission due to terbium out of the rest of the spectrum. This is possible thanks to the time-resolved emission of fluorescence (TREF). The integration of the fluorescence intensity from $t = 0.88$ ms after the lamp flash to $t = \infty$ measures the fluorescence intensity contribution of the long-lifetime components. In this way, the short-lifetime components due to the organic parts of the molecule have been eliminated I_{TREF} can be defined as

$$I_{TREF} = \frac{\int_{0.88ms}^{\infty} F(t)dt}{\int_{0}^{\infty} F(t)dt} \tag{7}$$

where $F(t)$ is the fluorescence intensity at time t after the excitation pulse. Figure 3 shows the TREF excitation and emission spectra of Pso–Tb. It appears clearly that the I_{TREF} of Pso–Tb is maximum for excitation wavelengths below 300 nm but displays a well-defined peak at 460 nm. It can be concluded that the part of the fluorescence spectra (Fig. 2) for excitation from 300 to 450 nm is due mainly to short-lifetime components (PAS, in fact). Furthermore, the TREF emission spectrum for excitation at 460 nm clearly shows the characteristic fluorescence peaks of terbium (490, 545, and 580 nm). Therefore, the best excitation wavelength is 460 nm; because Tb^{3+} has a maximum fluorescence intensity, short-lifetime components of the organic part are minimal and DNA no longer absorbs light at this wavelength. The best emission wavelength is 490 nm, where the contribution of the fluorescein fluorescence is weak. Indeed, fluorescein fluorescence will also show a long-lifetime component equal to terbium lifetime due to energy transfer from terbium (see below), which was used, for example, by Selvin *et al.*[17] to observe energy transfer between a terbium complex and an acceptor, both covalently bound to DNA.

The fluorescence lifetime of the terbium in this complex is 1.88 ms. It can be seen in Fig. 3 that for excitation at wavelengths under 300 nm, the terbium fluorescence lifetime decreases to about 0.7 ms, indicating the existence of a secondary deexcitation process for the terbium, possibly through a nonradiative energy transfer process to the psoralen moiety (this excitation region corresponds to the wavelength range where psoralen absorbs). The presence of a second lifetime below 300 nm can result from the presence of an other terbium complex which would not have the psoralen moiety, due to an

incomplete reaction during the synthesis. As this impurity cannot be covalently bound to DNA, it will be removed during the dialysis step and will thus not interfere with the energy transfer measurements. For excitation at 460 nm, only one lifetime is observed, so that no interfering deexcitation process occurs for this excitation wavelength. There is also an energy transfer from PAS to terbium. Indeed, if the PAS moiety is omitted during the synthesis of the complex, the fluorescence intensity of the terbium complex is greatly reduced. The PAS acts as a sensitizer of terbium fluorescence in Pso–Tb complex.

The quantum yield is defined as $\Phi = \tau/\tau_0$, where τ is the terbium lifetime in the complex and τ_0 is the intrinsic lifetime of terbium, in the absence of any nonradiative energy transfer. Stein *et al.*[18] showed that the τ_0 of terbium is 4.75 ms. The quantum yield of Pso–Tb is thus 39%. The overlap integral (J) with fluorescein is $1.53 \cdot 10^{-13}$ cm^3/(mol/L). The R_0 value for the transfer from terbium to fluorescein obtained from Eq. (4) is 47 Å.

Evidence for the Existence of an Energy Transfer Between Tb^{3+} and Fluorescein

Preliminary experiments were necessary in order to prove the existence of an energy transfer between the Pso–Tb complex and fluorescein. One way to do this is to observe a decrease in the intensity of fluorescence emission of the donor and an increase in the intensity of fluorescence emission of the acceptor when the acceptor concentration increases. This is possible only in the case where there exists an excitation wavelength where only the donor molecules absorb. Furthermore, the emission spectra of the donor and of the acceptor should be well separated. Unfortunately, in the case Pso–Tb → fluorescein, the fluorescein has a very wide absorption spectrum that totally overlaps the terbium absorption spectrum and the fluorescence emission spectra of both compounds occur in the same spectral region. So, a classical fluorescence emission spectrum cannot distinguish between the emission of directly excited fluorescein and fluorescein excited by energy transfer. Nevertheless, it is possible to distinguish these two contributions thanks to the time-resolved emission of fluorescence (TREF). Morrisson[19] showed that, in the case of energy transfer, the time-resolved fluorescence of the acceptor can be decomposed in a sum of two decreasing exponential terms: the first term, due to direct excitation, has a lifetime equal to the fluorescence lifetime of the acceptor in the absence of the donor, and the second term, due to the excitation through energy transfer, has a lifetime equal to the lifetime of the donor molecule. Using the TREF technique, the contribution to fluorescence of directly excited fluorescein can be eliminated. Figure 3 shows the TREF emission spectra of Pso–Tb in the presence of increasing fluorescein concentrations. The Tb^{3+} emission peaks at 490, 545, and 580 nm decrease, indicating that the excited terbium is transferring part of its energy to another molecule. Eventually, as the fluorescein concentration reaches $5 \cdot 10^{-5}$ mol/L, the Tb^{3+} peaks totally disappear and the emission spectrum becomes entirely due to fluorescein fluorescence. This long-lifetime emission spectrum of the fluorescein proves that the acceptor is excited by a long-lifetime donor. It can be concluded without any doubt that there is an energy transfer between the Pso–Tb complex and the fluorescein.

Energy Transfer $TbEDTA^- \rightarrow$ Fluospheres and Pso–Tb → Fluospheres

It was necessary to check that the energy transfer between terbium complexes and the Fluospheres happened in the fast diffusion limit of DERET. Indeed, the spheres are large, so that diffusion can be relatively slow. From a theoretical point of view, the FDL-DERET conditions are satisfied if $D\tau_0/d^2 > 1$. D is the translational diffusion coefficient, which, for a sphere, is equal to $D = kT/6\pi\eta a$ (η is the solvent viscosity and a the sphere radius).[20] The mean distance d (Å) between donor and acceptor can be estimated to be

$$d^3 = \frac{3}{4\pi} \frac{10^{30}}{[\text{Acceptor}]10^3 N_A}$$

The ratio $D\tau_0/d^2$ has been computed in Table I for the different Fluospheres. All Fluospheres seem to meet FDL-DERET conditions, except the 2470-Å Fluosphere. In practice, a plot of the reciprocal of terbium lifetime versus acceptor concentration must be linear in the FDL-DERET conditions [Eq. (5)] and the slope is equal to the dynamic transfer rate constant k_d. The rate constants for transfer between Fluospheres and $Tb(EDTA)^-$ and Pso–Tb have been determined. Figure 4 shows the dependence of the reciprocal of the terbium lifetime as a function of acceptor concentration. Transfer rate constants determined experimentally together with the linear correlation coefficient are collected in Table I. In all cases, the dependence is linear, except for the largest Fluosphere, which displays a poor correlation coefficient (especially with DNA and chromatin). The Fluospheres up to 977 Å can thus be used in FDL-DERET conditions for energy transfer with terbium complexes. The 2470-Å

Table I. FDL-DERET Condition, Number of Fluorescein Molecules on a Fluosphere, Total Electrical Charge of the Acceptor, and Transfer Rate Constants for Different Acceptor/Donor Couples and Correlation Coefficient for the Linear Regression of the Reciprocal of the Lifetime Versus the Fluorescein Concentration[a]

Acceptor				Fluorescent donor							
		Number of fluorescein molecules on the sphere	Total charge of the acceptor	Tb(EDTA)$^-$		Pso–Tb		Pso–Tb/DNA		Pso–Tb/Decondensed Chromatin	
Acceptor type	$D\tau_0/d^2$	(N_F)	(μC)	k_d (10^6 M^{-1} s^{-1})	Linear correlation coefficient	k_d (10^6 M^{-1} s^{-1})	Linear correlation coefficient	k_d (10^6 M^{-1} s^{-1})	Linear correlation coefficient	k_d (10^6 M^{-1} s^{-1})	Linear correlation coefficient
Fluorescein			$1.6 \cdot 10^{-13}$	22 ± 2	0.996	69 ± 11	0.965	31 ± 13	0.863	28 ± 2	0.997
Fluosphere											
d=14 nm	131.5	18	$4.1 \cdot 10^{-12}$	5.6 ± 0.4	0.992	21 ± 7	0.903	1.2 ± 0.1	0.993	12 ± 1	0.988
d=93 nm	19.8	$1.0 \cdot 10^4$	$1.4 \cdot 10^{-10}$	3.5 ± 0.3	0.977	10 ± 2	0.925	1.5 ± 0.1	0.994	14 ± 4	0.935
d=282 nm	6.5	$2.9 \cdot 10^6$	$3.0 \cdot 10^{-9}$	2.6 ± 0.1	0.995	10 ± 2	0.928	1.0 ± 0.1	0.987	5 ± 2	0.833
d=977 nm	1.9	$1.5 \cdot 10^8$	$4.8 \cdot 10^{-8}$	1.1 ± 0.1	0.984	4.4 ± 0.8	0.985	0.5 ± 0.3	0.997	2.1 ± 0.3	0.955
d=2470nm	0.7	$2.5 \cdot 10^9$	$1.78 \cdot 10^{-7}$	1.0 ± 0.1	0.973	6.8 ± 1	0.919	1.8 ± 1.5	0.5647	2.48 ± 0.01	0.798

[a]Pso–Tb concentration, 10^{-6} M; DNA and chromatin concentration, 10^{-4} M. Buffer: 10^{-3} M sodium cacodylate, pH 6.5. Excitation wavelength, 460 nm; emission wavelength, 490 nm.

Fluosphere diffuses too slowly to be in FDL-DERET condition, as theoretically predicted.

It can be seen from Table I that the transfer rate constant diminishes when the diameter of the acceptor particle increases, meaning that the larger the acceptor, the larger is the distance of closest approach [Eq. (6)]. Larger spheres have more difficulties in approaching the fluorescent donor.

In all cases, the rate constant for the transfer from Tb(EDTA)$^-$ is smaller than the corresponding constant for the transfer from Pso–Tb because of the difference of electrical charge on the complexes. The Tb(EDTA)$^-$ carries one negative charge. On the other hand, the Pso–Tb complex has a diazanonyl linker that contains two amino groups, which are both protonated at pH 6.5. These positive charges will screen the negative charge of the DTPA moiety (Fig. 1). The electrostatic repulsion between the Pso–Tb complex and the negatively charged Fluospheres will be reduced and thus the Pso–Tb complex will approach the Fluospheres more easily, resulting in an increase in the transfer rate constant.

Energy Transfer Pso–Tb/DNA → Fluospheres

Before probing chromatin with Pso–Tb, we wanted to check the effect on the transfer rate constant of an increase in salt concentration in the presence of both DNA and Fluospheres. The effect of salt on the system Pso–Tb/chromatin analyzed below should reflect changes in the transfer rate due to a modification of accessibility of the linker-DNA and not secondary effects, such as Fluosphere precipitation, charge neutralization, etc.

The transfer rate constants for the transfer from Pso–Tb/DNA to Fluospheres at a low salt concentration (1 mM sodium cacodylate) are collected in Table I. In all cases, the transfer rate constant is much smaller than from Pso–Tb free in solution to the corresponding sphere. Thus, the binding of Pso–Tb to DNA reduces its accessibility. This can be easily understood: the presence of the DNA helix causes a steric hindrance to the approach of the acceptor. Furthermore, DNA is negatively charged and produces a repulsion toward the negatively charged acceptor.

Figures 5B to D show no significant variation of the transfer rate constant with an increase in sodium chloride concentration for transfer between free Pso–Tb and Fluospheres or Pso–Tb/DNA and fluorescein or Fluospheres. A statistical test based on the "null hypothesis"[21] was used in order to check that the slope of the regression line was not significantly different from zero, indicating that there is no correlation between the energy transfer rate constant and the NaCl concentration. No precipitation of the Fluospheres was observed. Thus, the charge neutralization of the Fluospheres induced by the cations is not sufficient to increase the DNA accessibility or to allow sphere aggregation. We can thus be confident that no side effect can result during the increase in ionic strength in the case of the measurements described below. The increase in rate constant in the case of transfer from free Pso–Tb to fluorescein (Fig. 5A) results from a variation of the fluorescein absorption

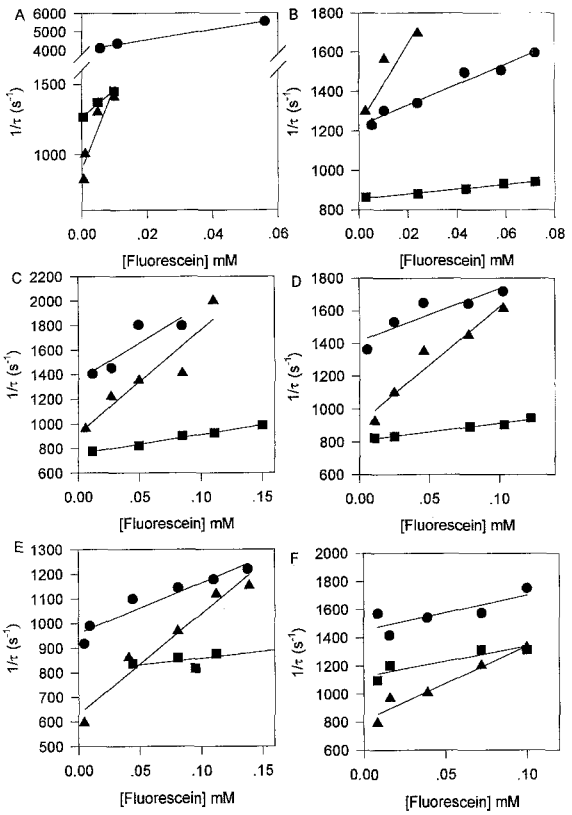

Fig. 4. Reciprocal of the fluorescence lifetime of Pso–Tb as a function of the fluorescein concentration (excitation, 460 nm; emission, 490 nm). Fluorescent donors: triangles, Pso–Tb, squares, Pso–Tb/DNA; circles, Pso–Tb/chromatin. Acceptors: (A) fluorescein; (B–F) Fluospheres with respective diameters of 14, 93, 282, 977, and 2470 nm.

spectrum as [NaCl] is increased, leading to a variation of the overlap integral, as already shown by Labarbe *et al.*[22]

Energy Transfer Pso–Tb/Chromatin → Fluospheres

The transfer rate constants from Pso–Tb complex covalently bound to linker-DNA in chicken erythrocyte chromatin to the Fluospheres at a low salt concentration (chromatin is in extended form) are given in Table I. The transfer rate constants are smaller than for the corresponding transfers from free Pso–Tb (except for the 93-nm Fluosphere). Thus, the fluorescent donor is more accessible when free in solution than when it is bound to chromatin. On the other hand, they are generally larger than for transfer from Pso–Tb bound to DNA. How can Pso–Tb bound to chromatin be more accessible than when it is bound to DNA? The presence of histone proteins should reduce the accessibility due to steric hindrances. As the histones are positively charged,[23] they

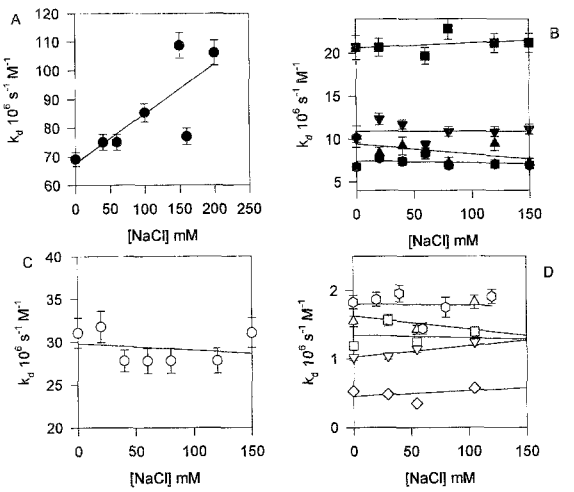

Fig. 5. Evolution of the dynamic transfer constant k_d as a function of the sodium chloride concentration. (A) Transfer from Pso–Tb to fluorescein. (B) Transfer from Pso–Tb to 14 nm (squares), 93 nm (up triangles), 282 nm (down triangles), 977 nm (diamonds), and 2470 nm (hexagons) Fluospheres. (C) Transfer from Pso–Tb/DNA to fluorescein. (D) Transfer from Pso–Tb/DNA to Fluospheres (same symbols as in B).

partially neutralize the negative charges of DNA, reducing the electrostatic repulsion of Fluosphere, which yields an increase in rate constant. It is interesting to note that the sensitivity of the FLD-DERET rate constant to electrostatic interactions, which has been used for example by Wensel *et al.*[12] to study the electrostatic properties of proteins, could give interesting information about the electrostatic field around the DNA or chromatin. The electrostatic interaction between DNA polyelectrolytes has indeed been at the center of an intense debate these last years.[24,25]

Chromatin condensation was induced by the addition of microvolumes of sodium chloride to a solution containing Pso–Tb/chromatin and Fluospheres. Widom[24] showed by electron microscopy and X-ray scattering that a sodium concentration above 50 m*M* will induce chromatin folding. The measure of the variation of terbium lifetime as a function of salt concentration allowed us to determine the variation of transfer rate constant during chromatin condensation (Fig. 6). Free fluorescein and the 14-nm Fluospheres showed no variation of transfer rate constant with salt concentration (Figs. 6A and B). Indeed, by applying the "null hypothesis" statistical test, only the decreases observed with the spheres larger than 93 nm are significant; in the case of fluorescein and the 14-nm Fluosphere, the slope of the regression line is not significantly different from zero, meaning that linker-DNA is still accessible to mol-

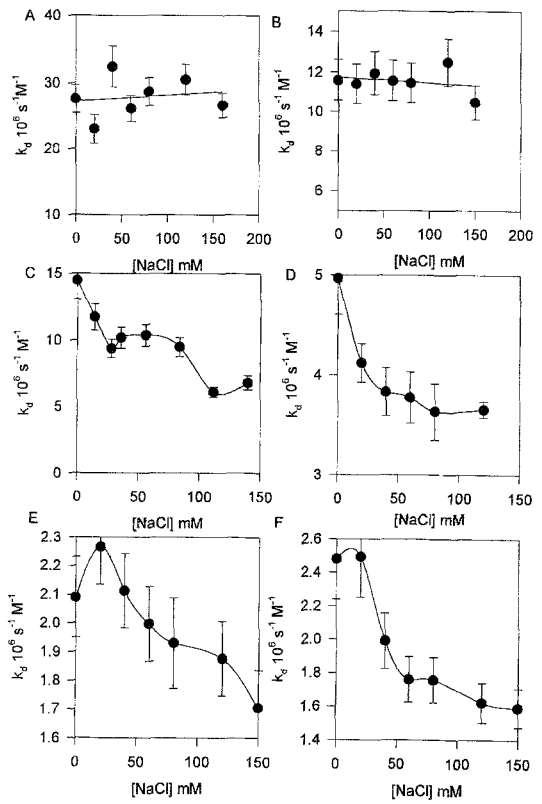

Fig. 6. Evolution of the dynamic transfer rate constant (circles) as a function of the sodium chloride concentration. The verticals bars are the estimated error on the transfer rate constant. Donor: Pso–Tb/chromatin. Acceptor: (A) fluorescein; (B–F) Fluospheres with respective diameters of 14, 93, 282, 977, and 2470 nm. Excitation, 460 nm; emission, 490 nm.

ecules up to a diameter of 14 nm even in the condensed structures of chromatin. With the Fluospheres of diameter 93, 282, 977, and 2470 nm, the general trend is a decrease, which is significantly larger than the experimental error, of the transfer rate constant as the sodium concentration increases. Thus, for molecules with a diameter superior to 14 nm, the accessibility of linker-DNA is reduced in the condensed structures of chromatin: acceptor can no longer approach the linker in the 30-nm fiber.

DISCUSSION

It is generally accepted that below 50 m*M* NaCl, chromatin is in an unfolded state. In early electron microscopy experiments, chromatin appeared to adopt an open zigzag structure 100 Å wide at low ionic strength.[25,26] When the sodium or magnesium concentrations were increased, respectively, over 50 m*M* or 200 μ*M*, chromatin took a more condensed structure called the 30-nm fiber.[23] Various models of chromatin fibers have been proposed. Finch and Klug[25] described the 30-nm fiber as a solenoid containing six nucleosomes per turn and a pitch of 110 Å. The exact orientation of the nucleosomes and the position of linker-DNA and its associated H1 histone, are not exactly known. Several models have been proposed. McGhee *et al.*[27] proposed that the linker was coiled around a helix the axis of which passes through the center of the nucleosomes, implying that the center of the 30-nm fiber is hollow. In the model proposed by Butler *et al.*,[28] linker-DNA makes a reverse loop between two successive nucleosomes in the center of the fiber. The cross-linker model proposed by Williams *et al.*[29,30] possesses nonsequential nucleosomes connected by transversal linkers passing through the center of the fiber. Woodcock *et al.*[31] proposed a two-start helical model where a zigzag fiber is compacted into a solenoid.

The chromatin appears now to have a loose three-dimensional structure, even at low salt concentrations. Scanning force microscopy of chromatin at a low salt concentration revealed that its structure is a loose array of nucleosomes with a diameter of about 34 nm.[32] When the salt concentration is increased, the chromatin gradually compacts nearly without any change in its diameter. Over 80 m*M* sodium, it adopts a compact irregularly segmented structure, much less regular than what was initially proposed in previous models.[32]

Variation of Linker-DNA Accessibility During Chromatin Condensation

Equation (6) allows us to compute the distance of closest approach (d) between DNA in the chromatin cylinder and the Fluosphere. From this equation, it is evident that a reduction of DNA accessibility (i.e., an increases in the distance of closest approach) will result in a decrease in the dynamic transfer constant k_d.

When the diameter of the Fluosphere probe is inferior to 14 nm, the accessibility is independent of sodium ion concentration, indicating no variation of linker-DNA accessibility for small molecules during condensation (Fig. 6). When the diameter of the probe is superior to 93 nm, a decrease in DNA accessibility is observed during chromatin condensation (Fig. 6). The decrease in accessibility can be due only to steric hindrance preventing the approach of the Fluosphere toward the linker-DNA as a result of the condensation process, and not to secondary effects, as no variation of accessibility is observed for naked DNA (Fig. 5). It should

be noted that an increase in salt concentration increases the screening of the negative charges of the DNA and Fluospheres, which increases the accessibility. As the observed effect is, on the contrary, a decrease in accessibility with increasing salt concentration, the effect of charge screening does not conflict, from a qualitative point of view, with the conclusion that the decrease in rate constant is due to chromatin condensation. However, it limits the quantitative aspects of the experiment, as it results in an underestimation of the minimal approach distance between donor and acceptor.

We conclude that the critical diameter for protein exclusion from compact chromatin structures must be between 14 and 93 nm. The critical diameter may be compared with the size of the RNA polymerase protein. Eukaryotic RNA polymerases consist of different subunits, the largest units typically having molecular weights of 200,000 and 140,000 daltons. There are 10 more units with a molecular weight ranging from 10,000 to 90,000 daltons.[33] The total RNA polymerase weighs approximately 500,000 daltons. The diameter of the polymerase can be estimated to be superior to 15 nm. The polymerase is thus sufficiently large to be kept away from the DNA in the condensed chromatin. It can be speculated that the exclusion could be partially responsible for the long-term repression of the genes in the condensed chromatin structures.

It is considered that chromatin condenses at 50 m*M* NaCl. However, our accessibility measurements show that the chromatin accessibility already decreases at 20 m*M* NaCl (Fig. 6). The accessibility decreases up to 150 m*M* NaCl. Thus, condensation is not an all-or-none process where a two-state equilibrium abruptly switches from the decondensed to the condensed state at a particular sodium concentration. The condensation must rather be considered as a gradual reorganization of the chromatin structure from an open to a more compact structure.

The location of the linker in the chromatin fiber has been the subject of intense debate during these last years. The observed decrease in linker accessibility indicates that the linker cannot be situated on the outside of the condensed fiber; otherwise, condensation would not lead to an increase in the distance of closest approach between Fluospheres and linker-DNA. Linker-DNA must be located somewhere inside the condensed structure. As histone H1 is bound to the linker-DNA,[34] this also means that H1 must be located inside the fiber, in agreement with previous fluorescence measurements made with labeled H5 histones,[35] neutron scattering measurements,[36] and micrococcal nuclease digestion.[32,37]

When the diameter of the probe is less than 14 nm, linker-DNA is equally accessible in condensed as in decondensed chromatin. Furthermore, the distance of closest approach of the 14-nm fiber is quite small, even smaller than the diameter of the chromatin fiber. Since the linker must be situated in the interior of the chromatin fiber, this means that there must be a way for small molecules to diffuse inside the chromatin fiber. This observation favors models of chromatin fiber in which there is a central cavity in the solenoid where small molecules are free to diffuse.

In conclusion,

(i) linker-DNA is situated inside the condensed chromatin fiber,
(ii) condensed chromatin prevents molecules with a diameter larger than 14 nm from approaching linker-DNA,
(iii) chromatin condensation is a gradual process, and
(iiii) models of chromatin fiber containing a central cavity seem to be the more likely.

APPENDIX

The Static Rate Constant for Transfer Between a Donor Molecule and a Sphere Uniformly Labeled with Acceptors

Equation (1) gives the expression of the static transfer rate constant between a donor molecule and an acceptor molecule. It is necessary to modify this expression for the case of a transfer between a donor (Pso–Tb) and a sphere uniformly labeled with acceptor molecules (Fluosphere). The probability that a transfer to the whole sphere occurs is equal to the sum of the probability of a transfer to each of the elementary volume elements dV of the sphere. The static transfer rate constant will be equal to (Fig. 7)

$$k_{2\text{Sphere}} = 8.7\cdot10^{23}\, J\kappa^2\Phi_0 n^{-4}\frac{1}{\tau_0}\int_{\text{VOLUME}} \rho(r)\frac{1}{r^6}dV$$

$$= 8.7\cdot10^{23}\, J\kappa^2\Phi_0 n^{-4}\frac{1}{\tau_0}\int_0^a \mathbf{r}'^2\, dr'$$

$$\int_0^{\pi} \rho(r)\,\frac{2\pi\sin(\theta)}{r^6}\,d\theta \qquad (8)$$

where J is the overlap integral between the emission spectrum of the donor and the absorption spectrum of the acceptor molecule, $\rho(r)$ is the density (molecule/Å^3) of acceptor at point r on the sphere, a is the radius of the sphere (Å), and $dV = dx\cdot dy\cdot dz$ is the volume element.

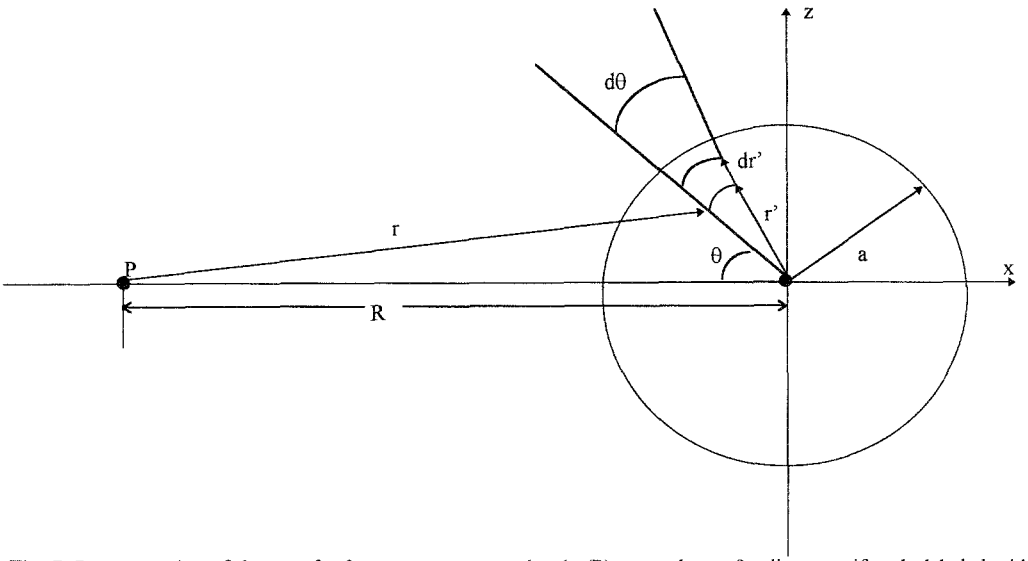

Fig. 7. Representation of the transfer from an acceptor molecule (P) to a sphere of radius a, uniformly labeled with acceptors.

The other parameters are shown in Fig. 7. The density of fluorescein molecules on the sphere is supposed to be constant.

It should be noted that the refractive index is not constant everywhere along the line joining the donor and the acceptor. Indeed, inside the sphere the refractive index is $n = 1.6$ for polystyrene, and outside $n = 1.33$ for water. Nevertheless, for simplicity, as the difference between the two indexes is small, we assume that the refractive index is 1.33 in the whole space, even inside the sphere.

As the overlap integral J corresponds to transfer to *one* acceptor molecule, all the constants in front of the integral can be collected in a term R_0^6/τ_0, where R_0^6 is the critical Förster distance for the transfer to *one* acceptor molecule.

Referring to Fig. 7 and using trigonometric relations, it is evident that

$$r^2 = r'^2 + R^2 - 2r'R\cos(\theta) \tag{9}$$

where R is the distance between the donor and the center of the sphere.

The transfer rate constant has to be computed for a constant donor–center of sphere distance, so that R is a constant. For any given value of r' (i.e., r' is constant), differentiation of Eq. (9) will give

$$\frac{\sin(\theta)d\theta}{r} = \frac{dr}{r'R}$$

The boundaries of integration are found in Eq. (9). If θ varies from 0 to π, r will vary from $R - r'$ to $R + r'$.

Equation (8) then becomes

$$k_{2\text{Sphere}} = \frac{R_0^6}{\tau_0}\frac{\rho}{R}2\pi\int_0^a \mathbf{r}'\,dr'\int_{R-r'}^{R+r'}\frac{dr}{r^5}$$

$$= \frac{R_0^6}{\tau_0}\frac{4}{3}\pi\rho a^3\frac{1}{[(R+a)(R-a)]^3}$$

The number N_F of acceptor molecules bound on a sphere is equal to

$$N_F = \frac{4}{3}\pi a^3\rho$$

The equation can be further simplified by the following approximation:

$$(R - a)(R + a) \cong R^2$$

The static rate constant can now be written as

$$k_{2\text{Sphere}} = \frac{R_0^6}{\tau_0}\frac{N_F}{R^6} \tag{10}$$

So the transfer between a donor molecule and a sphere uniformly loaded with N_F acceptor molecules can be approximated as happening between a donor and a sphere with all N_F acceptor molecules located at the center of the sphere.

The Dynamic Transfer Rate Constant for a Transfer Between a Donor Molecule and a Sphere Uniformly Labeled with Acceptor

The dynamic transfer rate constant is computed by integration of Eq. (10) for all positions and orientations of the donor and acceptor. In the case of a transfer be-

tween a donor located at the center of a cylinder (DNA) of radius R_d and an acceptor located at the center of a sphere (Fluosphere) of radius R_a, the dynamic transfer rate constant can be computed by a simple modification of the Wensel formula [11]:

$$k_{\text{dSphere}} = \frac{10^{-27} \cdot N_A \pi^2}{4\tau_0} \frac{R_0^6}{d^3} N_F = k_d N_F$$

where N_A is Avogadro's number and d (Å) the distance of closest approach ($d = R_d + R_a$). It must be noted that k_d is equal to the dynamic transfer rate constant for a transfer to one acceptor molecule located at the center of the same sphere. The advantage of uniformly labeled sphere is to increase the rate constant by a factor equal to the number of acceptor molecules loaded on the sphere, allowing the use of a lower sphere concentration and thus reducing the amount of light scattered by the spheres, making experimental observations easier.

The evolution of the fluorescence lifetime of the donor with sphere concentration will be given, in the FDL-DERET limit, by Eq. (5):

$$\begin{aligned} \frac{1}{\tau} &= \frac{1}{\tau_0} + k_{\text{dSphere}}[\text{Sphere}] \\ &= \frac{1}{\tau_0} + k_d N_F[\text{Sphere}] \\ &= \frac{1}{\tau_0} + k_d[\text{Acceptor}] \end{aligned}$$

Since each Fluosphere is labeled with N_F acceptor molecules, when using the fluorescein-labeled Fluospheres, in order to compare the dynamic transfer rate constant of spheres of different diameters (and consequently a different number of fluorescein molecules bound to them), it is important to compare the k_d constants (rather than the k_{dSphere} constant) for which the effect of N_F has been eliminated. Consequently, the dynamic rate constant will be determined by linear regression on $1/\tau$ versus [Fluorescein] (where [Fluorescein] = N_F [Sphere] is the total fluorescein concentration in solution).

ACKNOWLEDGMENTS

This work was supported by the Fonds National de la Recherche Scientifique (FNRS Aspirant status to R. Labarbe), a research fellowship from FRIA to S. Flock, and Research Grant ARC 91/95-152.

REFERENCES

1. G. Reuter, M. Giarre, J. Farah, J. Gausz, A. Spierer, and P. Spierer (1990) *Nature* **344**, 219–223.
2. J. C. Hansen and A. P. Wolffe (1992) *Biochemistry* **31**, 7977–7988.
3. R. T. Kamakaka and J. O. Thomas (1990) *EMBO J.* **9**, 3997–4006.
4. D. L. Bates., G. Butler, C. Pearson, and J. O. Thomas (1981) *Eur. J. Biochem.* **119**, 469–476.
5. J. Zlatanova (1990) *TIBS* **15**, 273–276.
6. P. R. Selvin (1995) *Methods in Enzymol.* **246**, 300–334.
7. A. Oser, M. Collasius, and G. Valet (1990) *Anal. Biochem.* **191**, 295–301.
8. A. Oser, W. K. Roth, and G. Valet (1988) *Nucleic Acids Res.* **16**, 1181–1196.
9. R. Marquet, P. Colson, A. M. Matton, and C. Houssier (1988) *J. Biomol. Struct. Dyn.* **5**, 839–857.
10. D. D. Thomas, W. F. Carlsen, and L. Stryer (1978) *Proc. Natl. Acad. Sci. USA* **75**, 5746–5750.
11. T. G. Wensel, C. H. Chang, and C. F. Meares (1985) *Biochemistry* **24**, 3060–3069.
12. T. G. Wensel and C. F. Meares (1983) *Biochemistry* **22**, 6247–6254.
13. G. D. Cimino, H. B. Gamper, S. T. Isaacs, and J. E. Hearst (1985) *Annu. Rev. Biochem.* **54**, 1151–1193.
14. W. Zhen, O. Buchardt, H. Nielsen, and P. E. Nielsen (1986) *Biochemistry* **25**, 6598–6603.
15. G. P. Wiesehahn, J. E. Hyde, and J. E. Hearst (1977) *Biochemistry* **16**, 925–932.
16. R. R. Sinden and P. J. Hagerman (1984) *Biochemistry* **23**, 6299–6303.
17. P. R. Selvin and J. E. Hearst (1994) *Proc. Natl. Acad. Sci. USA* **91**, 10024–10028.
18. G. Stein and E. Wurzberg (1975) *J. Chem. Phys.* **62**, 208–213.
19. L. E. Morrison (1988) *Anal. Biochem.* **174**, 101–120.
20. P. W. Atkins (1986) *Physical Chemistry*, Oxford University Press Oxford.
21. D. M. Himmelblau (1970) *Process Analysis by Statistical Methods*, Wiley, New York.
22. R. Labarbe, S. Flock, P. Colson, and C. Houssier (1994) *J. Fluoresc.* **4**, 315–318.
23. W. Saenger (1984) *Principles of Nucleic Acid Structure*, Springer Verlag, New York.
24. D. C. Rau, B. Lee, and V. A. Parsegian (1984) *Proc. Natl. Acad. Sci. USA* **81**, 2621–2625.
25. A. P. Lyubartsev and L. Nordenskiold (1995) *J. Phys. Chem.* **99**, 10373–10382.
24. J. Widom (1986) *J. Mol. Biol.* **190**, 411–424.
25. J. T. Finch and A. Klug (1976) *Proc. Natl. Acad. Sci. USA* **73**, 1897–1901.
26. F. Thoma, T. Koller, and A. Klug (1979) *J. Cell Biol.* **83**, 403–427.
27. J. D. McGhee, D. C. Rau, E. Charney, and G. Felsenfeld (1980) *Cell* **22**, 87–96.
28. P. J. G. Butler (1984) *EMBO J.* **3**, 2599–2604.
29. S. P. Williams, B. D. Athey, L. J. Muglia, R. S. Schappe, A. H. Gough, and J. P. Langmure (1986) *Biophys. J.* **49**, 233–248.
30. M. H. J. Koch, Z. Sayers, A. M. Michon, P. Sicre, R. Marquet, and C. Houssier (1989) *Eur. Biophys. J.* **17**, 245–255.
31. C. L. F. Woodcock, L. L. Y. Frado, and J. B. Rattnerf (1984) *J. Cell Biol.* **99**, 42–52.
32. J. Zlatanova, S. Leuba, H., G. Yang, C. Bustamante, and K. E. Van Holde (1994) *Proc. Natl. Acad. Sci. USA* **91**, 5277–5280.
33. B. Lewin (1985) *Genes*, Wiley, New York.
34. M. Noll and R. D. Kornberg (1977) *J. Mol. Biol.* **109**, 393–404.
35. G. Sarlet, S. Muller, and C. Houssier (1992) *J. Biomol. Struct. Dyn.* **10**, 35–47.
36. V. Graziano, S. E. Gerchman, D. K. Schneider, and V. Ramakrishnan (1994) *Nature* **368**, 351–354.
37. S. Leuba, H., J. Zlatanova, and K. E. Van Holde (1994) *J. Mol. Biol.* **235**, 871–880.